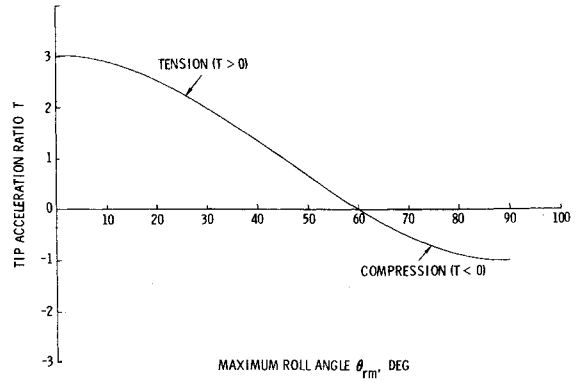

Fig. 3 Tip acceleration ratio T vs maximum roll angle θ_{rm} for a dumbbell in circular orbit.

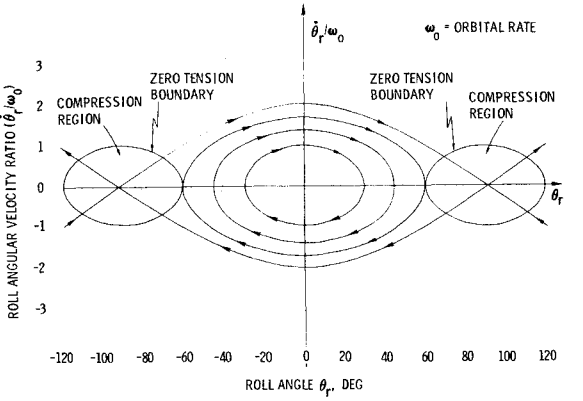

Fig. 4 Roll phase-plane diagram.

to maximum tension) is when $\theta_{rm}=0$ and it is zero when $\theta_{rm}=60$ deg. For $\theta_{rm}>60$ deg the array is in compression. The tension for a dumbbell with end masses M_{ant} is given by the equation

$$F=T(L\omega_0^2/2)M_{ant} \tag{3}$$

which is equivalent to Eq.(1) when $\sigma=\theta_r=\dot{\theta}_r=0$.

IV. Phase-Plane Analysis

The relationship between the roll angle and the roll rate can be obtained from the integration of the roll restoring angular acceleration expression

$$\ddot{\theta}_r=-2\omega_0^2\sin 2\theta_r \tag{4}$$

Multiplying Eq. (4) by $\dot{\theta}_r$ and integrating one obtains

$$\dot{\theta}_r^2/2=\omega_0^2\cos 2\theta_r+C \tag{5}$$

Closed trajectories in the phase plane $\dot{\theta}_r$ vs θ_r are separated from the unterminating ones by the solution of Eq. (5) which passes through $\theta_r=90$ deg, $\dot{\theta}_r=0$. For this solution, Eq. (5) is

$$(\dot{\theta}_r/\omega_0)^2=2(1+\cos 2\theta_r) \tag{6}$$

which is plotted in Fig. 4 along with other solutions corresponding to different initial values of $\dot{\theta}_r$ and θ_r. Also plotted is the case $T=0$ in Eq. (2) which delineates a region of compression in the $\dot{\theta}_r$, θ_r plane. These results show that the maximum roll angle must be less that 60 deg and should preferably be no greater than 30 deg. For the latter case the maximum tension will be 2/3 that at $\theta_{rm}=0$.

V. Flexibility Effects

The flexibility characteristics (natural frequencies and mode shapes) of the array play an important role in the design of the system. An insight into the nature of the normal modes can be obtained by examining those for a cable with and without tip masses. In general, the pitch and roll (in- and out-of-plane, respectively) librational modes are straight with 1.73 ω_0 and $2\omega_0$ frequencies in the linear range, respectively. The addition of a tip mass tends to increase the natural frequencies of all higher order modes.[4] It may thus be concluded that the array should maintain a straight (linear) configuration in a rolling librational mode up to 30 deg maximum angle.

VI. Summary and Conclusions

A concept for a gravitationally stabilized satellite solar power station in orbit has been described. The system consists of an array of solar cells feeding electric energy to a microwave antenna at the end of an Earth-pointing cable. Received power at the ground is in the 5000 to 10,000 MW range. The principal advantages of this concept are that 1) no excessively large structural subassemblies are required and 2) passive, long-life attitude control for the array is used. This concept separates the conventional very large solar flux collection assemblies into individual segments mutually connected by a gravitationally stabilized power distribution cable. Other desirable characteristics of the system are a gravitationally induced tension in the array and quite substantial restoring torques about the pitch and the roll axes. Rolling motion prevents the mutual shading of the array elements at the equinoxes.

Further studies to optimize the system parameters such as the size, shape, mass, and power are required, however, to more fully assess the feasibility and cost effectiveness of this concept.

References

[1]P.E. Glaser, "Evolution of the Satellite Solar Power Station (SSPS) Concept," *Journal of Spacecraft and Rockets*, Vol. 13, Sept. 1976. pp. 573-576.

[2]P.E. Glaser et al, "Feasibility Study of a Satellite Solar Power Station," NASA CR-2357, Feb. 1974.

[3]ECON Inc., "Space-Based Solar Power Conversion and Delivery Systems Study," Report No. 76-145-IB, March 31, 1976.

[4]G.B. Andeen, "Orbital, Attitude, and Deployment Considerations for a Passive Space Array," Stanford Research Institute Report No. 5, Dec. 1975.

Simple Algorithm for Intersecting Two Conical Surfaces

Carl Grubin*
Northrop Corporation, Hawthorne, Calif.

A PROBLEM of recurring interest in space mechanics is determining the intersection of two conical surfaces. For example, measuring the angle between a known star reference and an unknown vector locates the vector on a cone whose axis is the star line and whose semivertex angle is the measured angle. A second simultaneous measurement using another star locates the vector on a second cone. Obviously the vector lies at the intersection(s) of the two cones. This paper develops a simple algorithm for determining the intersection.

Analysis

Designate unit vectors along the cone axes as $\bar{e}_1$, $\bar{e}_2$, respectively. The angles between $\bar{e}_1$, $\bar{e}_2$ and the unknown

Received Nov. 11, 1976; revision received Nov. 29, 1976.
Index categories: Spacecraft Attitude Dynamics and Control; Spacecraft Navigation, Guidance, and Flight-Path Control Systems.

*Engineering Specialist, Electronics Division. Associate Fellow AIAA.

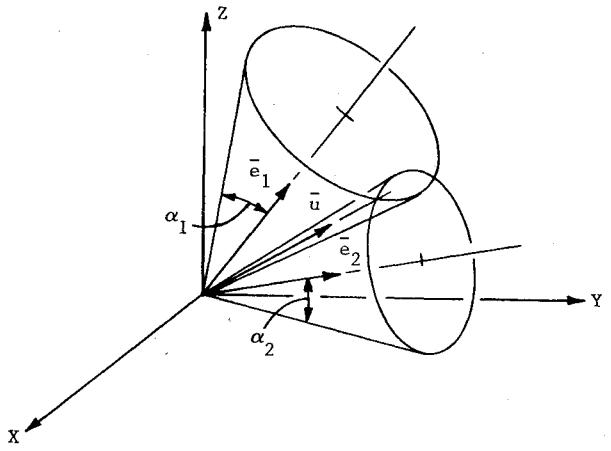

Fig. 1 Geometry.

vector $\bar{u}$ are measured as α_1, α_2, respectively. The problem is to determine $\bar{u}$ (Fig. 1).

Since $\bar{e}_1$, $\bar{e}_2$ are not parallel, a system of base unit vectors consisting of $\bar{e}_1$, $\bar{e}_2$ and $\bar{n}=(\bar{e}_1\times\bar{e}_2)\ /\ |\bar{e}_1\times\bar{e}_2|$ can be introduced. Thus, let $\bar{u}$ be expressed as

$$\bar{u}=\bar{e}_1 x+\bar{e}_2 y+\bar{n}z \tag{1}$$

where x, y, z are unknowns.

From Eq. (1) and the given data

$$\bar{u}\cdot\bar{e}_1=x+y\cos\theta=\cos\alpha_1 \tag{2a}$$

$$\bar{u}\cdot\bar{e}_2=x\cos\theta+y=\cos\alpha_2 \tag{2b}$$

where $\cos\theta=\bar{e}_1\cdot\bar{e}_2$, and θ is the angle between $\bar{e}_1$ and $\bar{e}_2$.

Solving Eqs. (2) for x, y

$$x=[\sin^2\theta]^{-1}(\cos\alpha_1-\cos\theta\cos\alpha_2) \tag{3a}$$

$$y=[\sin^2\theta]^{-1}(\cos\alpha_2-\cos\theta\cos\alpha_1) \tag{3b}$$

The $\bar{n}$ component, z, is determined from $\bar{u}\cdot\bar{u}=1$. This gives

$$z=\pm(1-x^2-y^2-2xy\cos\theta)^{1/2} \tag{4a}$$

An equivalent expression is

$$z=\pm(1-x\cos\alpha_1-y\cos\alpha_2)^{1/2} \tag{4b}$$

There are two solutions for z corresponding to $\bar{u}$ lying on one side or the other of the $\bar{e}_1$, $\bar{e}_2$ plane. Additional information is required to resolve this ambiguity. The general solution to the intersection problem is thus given by Eq. (1) with x,y, determined by Eqs. (3) and z by Eq. (4a) or (4b). Observe that for calculation purposes, $\bar{e}_1$, $\bar{e}_2$ and $\bar{n}$ are ultimately expressed in terms of some orthogonal inertial unit vectors.

The solution for z can be verified for the special case where $\bar{u}$ happens to be coplanar with $\bar{e}_1$, $\bar{e}_2$. This can occur in the following circumstances: 1) cones are externally tangent, in which case $\theta=\alpha_1+\alpha_2$; and 2) cones are internally tangent, in which case a) $\theta=\alpha_1-\alpha_2>0$, or b) $\theta=\alpha_2-\alpha_1>0$. For all cases, the solutions can be expressed as

$$x=\pm\frac{\sin\alpha_2}{\sin(\alpha_1\pm\alpha_2)}$$

$$y=\pm\frac{\sin\alpha_1}{\sin(\alpha_2\pm\alpha_1)}$$

$$z=0$$

where the + signs are used for case (1), and the minus signs for both cases (2).

A Simple Scale Length for Shocks about Transverse Gas Jets

D. W. Harvey*
McDonnell Douglas Astronautics Company, Huntington Beach, Calif.

Nomenclature

E = rms error
R = scale length; radius of shock-correlating sphere or cylinder (Fig. 1)
x,y = coordinate system of Ref. 2 (see Fig. 1)
X,Y = nozzle-centered coordinate system (Fig. 1)
X_{ref} = location of shock-correlating sphere or cylinder (Fig. 1)

WHEN a gas jet is injected transversely into a supersonic stream, one of the most prominent and easily measured features produced is the shock about the jet. This shock characterizes the interaction between the jet and the stream. The physical scale of the interaction is of substantial interest. This Note describes a simple method of deriving a scale length from experimental shock shapes.

The method is an extension of that reported by Kallis.[1] It is based on the assumption that the shock about a jet is sufficiently similar to that about a sphere or cylinder so that it can be characterized by a single scale length, the radius of the sphere or cylinder. Although not necessarily intuitively appealing, this assumption is a good one, as will be discussed below.

The essence of the method is that the shock shape expressions developed by Billig[2] are fit, in a least-squares sense, to the experimental shock shape data. Since neither the streamwise location nor the scale length R is known, this fit is a two-parameter one. It is done by assuming a location X_{ref} (see Fig. 1) and calculating a scale length R_i for each data point using Billig's shock shapes, which are of the form $X=f(y,R)$, inverted to give $R=g\ (x,y)$. The root mean square error is then

$$E(X_{\text{ref}})=\frac{1}{N}\left[\sum_{i=1}^{N}\left(\frac{R_i}{\langle R\rangle}-1\right)^2\right]^{1/2}$$

where $\langle R\rangle$ is the average over all N data points. It remains only to minimize E by proper (e.g., Newton-Raphson) adjustment of R. When this is done, $\langle R\rangle=R$, the desired scale length. The extension beyond Kallis' work[1] consists of determining X_{ref} from the fit, rather than directly estimating it from the photographs. The latter method requires visual extrapolation and is believed to induce unnecessary error.

Data from 26 shock-tunnel tests have been analyzed. Test conditions are given by Harvey et al.[3] The slot nozzles used are of 10-to-1 aspect ratio, transverse to the stream. Some results for a typical run are shown in Figs. 2 and 3. In Fig. 2, the actual points obtained from the shock are shown. They extend a considerable distance downstream and thus provide a reasonably critical test of the effect of obstacle shape. This downstream distance is typical for all runs. For each point, the calculated values of R_i are shown for three values of X_{ref}. The central one of these three values is the minimum error value. It is clear that, for this value of X_{ref}, there is no systematic variation of R with downstream distance; this

Received Oct. 18, 1976; revision received Dec. 7, 1976.
Index categories: Shock Waves and Detonations; Jets, Wakes, and Viscid-Inviscid Flow Interactions.
*Senior Engineer/Scientist.